Drosophila Spectrin: the Membrane Skeleton during Embryogenesis

Thomas C. Pesacreta, Timothy J. Byers, Ronald Dubreuil, Daniel P. Kiehart, and Daniel Branton

Department of Cellular and Developmental Biology, The Biological Laboratories, Harvard University, Cambridge, Massachusetts 02138

Abstract. The distribution of alpha-spectrin in *Drosophila* embryos was determined by immunofluorescence using affinity-purified polyclonal or monoclonal antibodies. During early development, spectrin is concentrated near the inner surface of the plasma membrane, in cytoplasmic islands around the syncytial nuclei, and, at lower concentrations, throughout the remainder of the cytoplasm of preblastoderm embryos. As embryogenesis proceeds, the distribution of spectrin shifts with the migrating nuclei toward the embryo surface so that, by nuclear cycle 9, a larger proportion of the spectrin is concentrated near the plasma membrane. During nuclear cycles 9 and 10, as the nuclei reach the cell surface, the plasma membrane-associated spectrin becomes concentrated into caps above the somatic nuclei. Concurrent with the mitotic events of the syncytial blastoderm period, the spectrin caps elongate at interphase and prophase, and divide as metaphase and anaphase progress. During cellularization, the regions of spectrin concentration appear to shift: spectrin increases near the growing furrow canal and concomitantly decreases at the embryo surface. In the final phase of furrow growth, the shift in spectrin concentration is reversed: spectrin decreases near the furrow canal and concomitantly increases at the embryo surface. In gastrulae, spectrin accumulates near the embryo surface, especially at the forming amnioproctodeal invagination and cephalic furrow. During the germband elongation stage, the total amount of spectrin in the embryo increases significantly and becomes uniformly distributed at the plasma membrane of almost all cell types. The highest levels of spectrin are in the respiratory tract cells; the lowest levels are in parts of the forming gut. The spatial and temporal changes in spectrin localization suggest that this protein plays a role in stabilizing rather than initiating changes in structural organization in the embryo.

ALTHOUGH a number of genes and gene products that specify and regulate *Drosophila* embryogenesis have been identified, understanding of developmental processes also requires knowledge of components that are mechanistic effectors of shape transformation, membrane domain formation, and cell division. Because these events in *Drosophila* are closely coordinated with the changing patterns of actin, myosin, and tubulin localization (Warn et al., 1984; Warn and Magrath, 1983; Karr and Alberts, 1986; Young, P. E., T. C. Pesacreta, and D. P. Kiehart, manuscript in preparation) and are specifically inhibited by microtubule and microfilament perturbants (Foe and Alberts, 1983; Zalokar and Erk, 1976; Warn et al., 1987), it is clear that cytoskeletal components play a major role in fly embryogenesis.

Spectrin, a cytoskeletal component that may be important in the function of membrane domains (Tokuyasu et al., 1979; Lazarides et al., 1984; Nelson and Veshnock, 1987) and that contributes to determination of shape and shape transformations in mammalian erythrocytes (Elgsaeter et al., 1986), is found in many eukaryotes, including *Drosophila* (Dubreuil et al., 1987). Because spectrin may interact with microfilaments (Glenney et al.. 1982), microtubules (Ishikawa et al., 1983; Sobue et al., 1987), and intermediate filaments (Langley and Cohen, 1986), and can be associated into a membrane skeleton near the cytoplasmic surface of the plasma membrane (for reviews see Bennett, 1985; Marchesi, 1985), it may be mechanistically involved in coordinating aspects of cytoskeletal function during *Drosophila* embryogenesis.

Spectrin distribution in insects has not been previously investigated, and spectrin distribution during embryogenesis is known only for mice (Sobel and Alliegro, 1985) and sea urchins (Schatten et al., 1986). As part of a broader investigation of the role of spectrin in nonerythroid cells, we have produced and characterized several antibody probes that are specific for *Drosophila* alpha-spectrin (Dubreuil et al., 1987; Byers et al., 1987). Here we use these probes to localize spectrin in developing *Drosophila* embryos and to analyze spectrin accumulation. Wherever possible we have related our observations on spectrin to other studies that have investigated the localization of actin during embryogenesis.

© The Rockefeller University Press, 0021-9525/89/05/1697/13 $2.00

Our results show that *Drosophila* eggs contain a substantial pool of maternal spectrin that undergoes dynamic changes in distribution during early *Drosophila* embryogenesis. After gastrulation, new synthesis is detected and spectrin is distributed near the plasma membrane of nearly all the cells of the postblastoderm embryo. The distribution of spectrin differs, in many cases, from that of actin.

Materials and Methods

Collection of Embryos

Embryos of *Drosophila melanogaster* (Canton-S) were grown at 25°C on grape juice-agar plates with yeast food. 1 h before placing a collection plate in a *Drosophila* cage, a fresh plate was introduced to stimulate deposition of any advanced embryos the females may have retained. 1 h later, this fresh plate was discarded and replaced with the actual collection plate. To harvest specific development stages the collection plate was removed from the population cage after 30–60 min and left at 25°C to develop as necessary.

Antibodies

Polyclonal rabbit serum 905 specific for *Drosophila* alpha-spectrin fusion protein 9a, as characterized in Byers et al. (1987), and preimmune serum collected from the same rabbit were used at 1:2,000 dilution for immunoblots or at 1:1,000 for immunolocalization. This antiserum is referred to as polyclonal antispectrin antibody or polyclonal antibody. In most cases, the polyclonal antibody was used after affinity purification on nitrocellulose strips (Olmsted, 1981) containing either purified spectrin from *Drosophila* S-3 cells (Dubreuil et al., 1987) or alpha-spectrin fusion protein 9a. Both purifications yielded antibodies that labeled embryos in a pattern identical to the antispectrin serum. For some experiments, monoclonal antibody M10-2, which is specific for alpha-spectrin in *Drosophila* S-3 cells (Dubreuil et al., 1987), was used in place of the polyclonal antibody. Culture supernatant from the clone was diluted 1:1 for use, whereas ascites fluid was diluted 1:50. Both preparations gave results which were qualitatively identical to the polyclonal antispectrin antibody in double-labeling experiments. Antibody specificity was further evaluated by preadsorbing the polyclonal antispectrin antibody to a nitrocellulose blot containing the fusion protein 9a produced from a pEV vector. In not one case did solutions that had been preadsorbed with the fusion protein produce the staining patterns described for antispectrin antibodies: only background equivalent to that seen with preimmune serum was observed. Antiserum adsorbed with proteins from *Escherichia coli* carrying the pEV plasmid without the 9a insert gave the same staining as nonadsorbed antibody.

As an actin probe, a monoclonal antiactin antibody diluted 1:100 (Lessard, 1988) was used. This antibody reacted with *Drosophila* actin on Western blots (data not shown). Although this antibody generally stained actin in cells, it failed, for some unexplained reason, to react with actin in the furrow canal region during cellularization. To analyze actin in this region, rhodamine phalloidin (0.33 μg/ml; Molecular Probes, Inc., Eugene, OR) was used.

Fixation for Microscopy

Embryos were placed in rinse solution (86 mM NaCl, 0.05% Tween-20, 10 mM NaN_3), dechorionated in 2.63% sodium hypochlorite (50% Clorox) for ~1.5 min, sedimented (table-top centrifuge; 30 s at 500 rpm), resuspended three times in rinse solution, and fixed at room temperature.

Because the vitelline envelope is impermeable to standard formaldehyde fixative solution, solutions similar to those in Karr and Alberts (1986) were used. Paraformaldehyde was stirred into a 100-mM solution of Pipes buffer, pH 7.3, at 80°C and brought to a final concentration of 2.5% (wt/vol) formaldehyde, 100 mM Pipes, 1 mM EGTA, 1 mM $MgCl_2$, 1 mM NaN_3, pH 6.9, adjusted with KOH. 10 ml of this solution was mixed with 5 ml of heptane and gently agitated for 5 min. For initial fixation, embryos were incubated in this solution with gentle tumbling at room temperature for 20 min. To remove the vitelline envelopes, the embryos were transferred to 100 ml of a second fixative (90% methanol, 50 mM EGTA, and an equal volume of heptane) in an Erlenmeyer flask. With intermittent agitation over a period of 10–20 min, many of the embryos sank; these were rinsed three times in 100% methanol (5 min each), once in 1:1 PBS (136 mM NaCl, 10 mM Na_2HPO_4/NaH_2PO_4, 2.5 mM KCl, pH 7.4)/methanol, three times in PBS, (5 min each), and either used immediately or stored at 4°C overnight.

Embryos to be incubated with rhodamine-phalloidin were not exposed to the second fixative. Instead, the vitelline envelope was removed with tungsten needles, and the embryos were put back into the aqueous component of the first fixative for 1 h.

For cryosectioning, embryos were fixed using the two-stage procedure, incubated in gradually increasing concentrations (10, 30, and 50%) of enzyme grade sucrose (Bethesda Research Laboratories, Gaithersburg, MD) in PBS at 4°C over several hours, mounted in O. C. T. (Miles Laboratories, Naperville, IL), frozen in dry ice, sectioned at a thickness of 5 μm on a Minotome (International Equipment Co., Needham Heights, MA), and mounted on glass slides coated with 1% gelatin dissolved in 0.1% chromium potassium sulfate.

To determine whether embryos lost spectrin during fixation, we measured the amount of spectrin lost to all preparative solutions using quantitative immunoblots. Duplicate groups of 100 embryos were collected at random from a single 10-h collection plate which included a wide range of developmental stages. The embryos were fixed as usual and then processed through all the usual solutions as for immunofluorescence (but without the addition of antibodies). All of the solutions through which the embryos had passed were combined and lyophilized. The amount of spectrin in the combined lyophilized solution residues, the fixed embryos, and an equal number of unfixed embryos was measured in quantitative immunoblots (see immunoblot method below). No spectrin was detected in the combined, concentrated, solution residue from 100 embryos even though the total spectrin in just one unfixed embryo contained more than the minimum amount of spectrin needed for detection. The fixed embryos retained ~70% of their spectrin immunoreactivity after having passed through all the usual preparative and staining solutions used to prepare the embryos for immunofluorescence microscopy. Thus little, if any, spectrin was lost to the solutions used during fixation and preparation for immunomicroscopy, although the spectrin retained by the embryos may have lost up to 30% of its immunodetectability as a consequence of the combined fixation steps.

Immunofluorescence

Whole mounts for immunocytochemistry were incubated in 25% goat serum in PBS for 30–60 min, briefly rinsed in incubation buffer (5% goat serum or newborn calf serum, 0.1% Tween-20, 10 mM NaN_3, in PBS) and then incubated in primary antibody diluted with incubation buffer for 1–3 h at room temperature or overnight at 4°C. During all incubations, the embryos were agitated by gentle tumbling. Unless stated otherwise, the figures in this paper illustrate results obtained with affinity-purified polyclonal antispectrin antibody. After rinsing in incubation buffer three times (30 min each), embryos were incubated in secondary antibody (FITC-labeled goat anti-rabbit or rhodamine-labeled anti-mouse antibody) for 1–2 h at room temperature, rinsed in buffer as before, rinsed twice in PBS (5 min each), and stained with Hoechst 33258 (0.5 μg/ml in PBS) for 15–30 min. Finally, embryos were rinsed in PBS twice and mounted in a mixture of 80% glycerol in PBS (pH 7.4), 1 mM NaN_3, and 1 mg/ml *p*-phenylenediamine.

Microscopy

A Zeiss microscope with epifluorescence optics was used. Embryos were routinely photographed using 100×, 40×, and 16× lenses. During the last stage of this research, a scanning confocal microscope (Bio-Rad Laboratories, Cambridge, MA) was used.

The precise developmental stage of each embryo was determined using at least one of several criteria. A high-resolution Nomarski image (using a 63×, 1.3 NA, Planapo lens) was sufficient to identify important features such as pole buds, pole cells, and furrows during cellularization and gastrulation; Hoechst staining was used to determine mitotic phase and number of nuclei per unit area at the embryo surface. The number of nuclei per unit area unambiguously defined the number of mitotic cycles through which the nuclei had gone.

Nomenclature

We adhered to the terminology of Foe and Alberts (1983) to describe the nuclear cycles: each nuclear cycle begins with the start of interphase and ends with the conclusion of mitosis. The timing given for each stage is that observed under our conditions.

When describing structures near the plasma membrane, we used the perspective of the plasma membrane being "above" the cytoplasm. "Apical" refers to the region of each cell that is or was nearest to the embryo surface during the cellular blastoderm stage. This study has analyzed the distribution of only the alpha chain of spectrin. Thus, "spectrin" refers only to alpha-spectrin. (Work using antibodies against the beta chain of *Drosophila*

spectrin has been initiated, but there is no evidence that the two chains are differently localized in the early embryo.) "Caps" refer to concentrations of spectrin or actin that are associated with the plasma membrane.

Quantitative Immunoblots

The total amount of spectrin per embryo was measured at different stages during embryogenesis. Because no system of collection was available that adequately synchronized development among populations of embryos, embryos were individually examined with a dissecting microscope to determine their stage of development. The following stages were defined by convenient morphological criteria that could be visualized in a dissecting microscope. The approximate age of the embryo (indicated in parentheses) is an estimate, based on normal development at 25°C (Campos-Ortega and Hartenstein, 1985): (*a*) pole cells absent (0–60 min); (*b*) pole cells present (60–120 min); (*c*) ongoing cellularization or amnioproctodeal invagination in external position (120–220 min); (*d*) amnioproctodeal invagination not visible, with the cephalic furrow the major external feature (220–260 min); (*e*) anterior segmentation evident (320–440 min); (*f*) segmentation prominent over almost the entire length of the embryo, with germband shortening (440–560 min); (*g*) clypeolabral shortening (560–620 min); and (*h*) midgut folded into a linear array of segments (780–960 min).

Embryos were dechorionated in 50% bleach and placed in rinse solution for microscopic inspection. Three samples, staged as described above, with eight embryos per sample, were collected for each developmental stage. Homogenization buffer was prepared by placing 20 μl of 5× SDS-PAGE

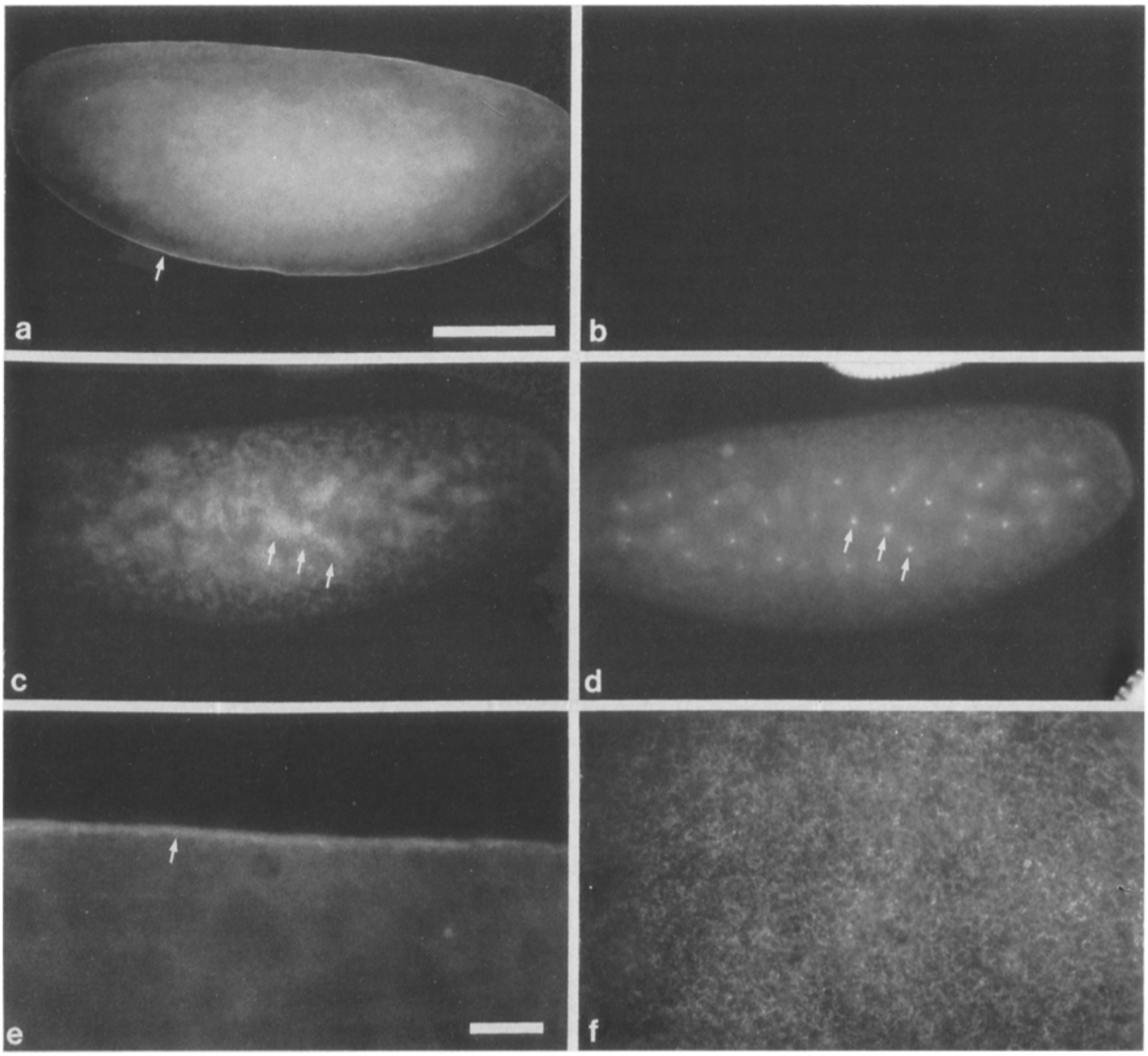

Figure 1. Spectrin in preblastoderm embryos. (*a*) Whole mount of a nuclear cycle 2 embryo, parasagittal optical section. Spectrin fluorescence is visible at the plasma membrane (*arrow*) and throughout the central regions of the embryo. (*b*) Whole mount of a nuclear cycle 7 embryo, optical section, labeled with preimmune serum (photographic conditions identical to *c*). (*c*) Spectrin fluorescence from whole mount of nuclear cycle 7 embryo, optical section, double labeled with antispectrin serum and Hoechst 33258. Because the optical section shown is not parasagittal, spectrin fluorescence at the plasma membrane is not visible in the photograph, although spectrin fluorescence was evident at the plasma membrane and is seen concentrated in cytoplasmic islands (*arrows*) that surround nuclei (shown in *d*). (*d*) Same as *c*, but illuminated to visualize Hoechst 33258 staining. The nuclei are grouped near the longitudinal axis of the embryo in a pattern that resembles that of the spectrin-containing cytoplasmic islands shown in *c* (*arrows*). (*e*) Same embryo as *a*, at higher magnification. Parasagittal optical section of the plasma membrane and associated spectrin (*arrow*). (*f*) Surface view of embryo in *a*. Bars: (*a–d*) 100 μm; (*e* and *f*) 10 μm. (Except where serum is specified, all of the figures in this paper show fluorescence due to binding of affinity-purified antispectrin antibody. Binding was detected with secondary antibody as described in Materials and Methods.)

sample buffer (250 mM Tris base adjusted to pH 6.8 with H_3PO_4, 347 mM SDS, 5.43 M glycerol, and 0.2 mg/ml bromphenol blue), 10 μl of 1 M dithiothreitol, and 1 μl of 100 mM PMSF from an isopropanol stock solution into a 1.5-ml polypropylene tube which was closed and then heated for 1 min in a boiling water bath. Eight embryos in 10 μl of rinse solution were added and homogenized with 30 strokes of a warm steel homogenizer. 50 μl of boiling, distilled water was washed over the homogenizer tip into the polypropylene tube, so that the total volume added to each sample was at most 90 μl. The mixture was heated in the closed tube for 20 min at 68°C, frozen in liquid nitrogen, and stored at −25°C. Upon thawing, each tube contained 65–70 μl; presumably, some liquid had been retained on the homogenizer or had been evaporated during heating.

The homogenates were electrophoresed on 8% acrylamide/0.08% bisacrylamide gels, quantitatively transferred to nitrocellulose, and immunostained with polyclonal antibody and alkaline phosphatase-coupled secondary antibody as described by Dubreuil et al., (1987). The gel lanes were each loaded with homogenate volumes representing known numbers of embryos, and the alkaline phosphatase reaction product on the immunoblots was quantified using the reflectance mode of a scanning densitometer (GS 300; Hoefer Scientific Instruments, San Francisco, CA). Preliminary experiments were performed to determine the range over which the amount of alkaline phosphatase reaction product was linearly related to the amount of homogenate added. The loading of gel lanes was adjusted within this range. The absolute amount of spectrin on the blots was estimated by comparison with a standard curve established with samples containing known amounts of *Drosophila* alpha-spectrin. The number of cells in a late stage embryo (i.e., an embryo which had completed the three major postblastoderm mitoses) was estimated to be 40,000, since there are ~5,000 cells in a cellular blastoderm embryo (Campos-Ortega and Hartenstein, 1985).

Results

Nuclear Cycles 1 through Metaphase, Nuclear Cycle 9 (from ~0 to 70 min): Spectrin Is Concentrated near the Plasma Membrane and Diffusely Distributed in the Cytoplasm

During the early period of preblastoderm embryogenesis, the nuclei divide eight times, beginning their movement to the embryo surface at the end of nuclear cycle 7 (for a description of embryogenesis see Campos-Ortega and Hartenstein, 1985). During this period, spectrin is concentrated subjacent to the plasma membrane (Fig. 1, *a* and *b*), in microtubule-rich regions (Karr and Alberts, 1986) that surround nuclei in the interior of the early syncytial embryo (Fig. 1, *c* and *d*), and, more diffusely, throughout the remaining embryo cytoplasm (Fig. 1, *a*, *c*, and *e*). Although spectrin appears as a continuous band near the plasma membrane in sagittal optical sections (Fig. 1 *e*), face views show that it forms an apparently random reticulum near the entire surface of each embryo (Fig. 1 *f*). The distribution of spectrin shows no evidence of being correlated with the radial migration of the nuclei from the center of the embryo to the surface and is not obviously polarized with regard to the dorsi-ventral or anterior-posterior axes of the early embryo. At a variable time during nuclear cycle 9, spectrin begins to redistribute into caps near the plasma membrane (see below).

Nuclear Cycle 9 through Interphase of Nuclear Cycle 10 (from ~70 to 85 min): Spectrin Caps Form

During this period, the somatic nuclei complete their migration from the inner regions of the embryo and come to lie within ~2.5 μm of the plasma membrane. Interphase of nuclear cycle 10 marks the beginning of the syncytial blastoderm period. During nuclear cycle 9, spectrin becomes concentrated into caps near the plasma membrane (Fig. 2 *a*), comparable to the caps of actin that also overlie the nuclei

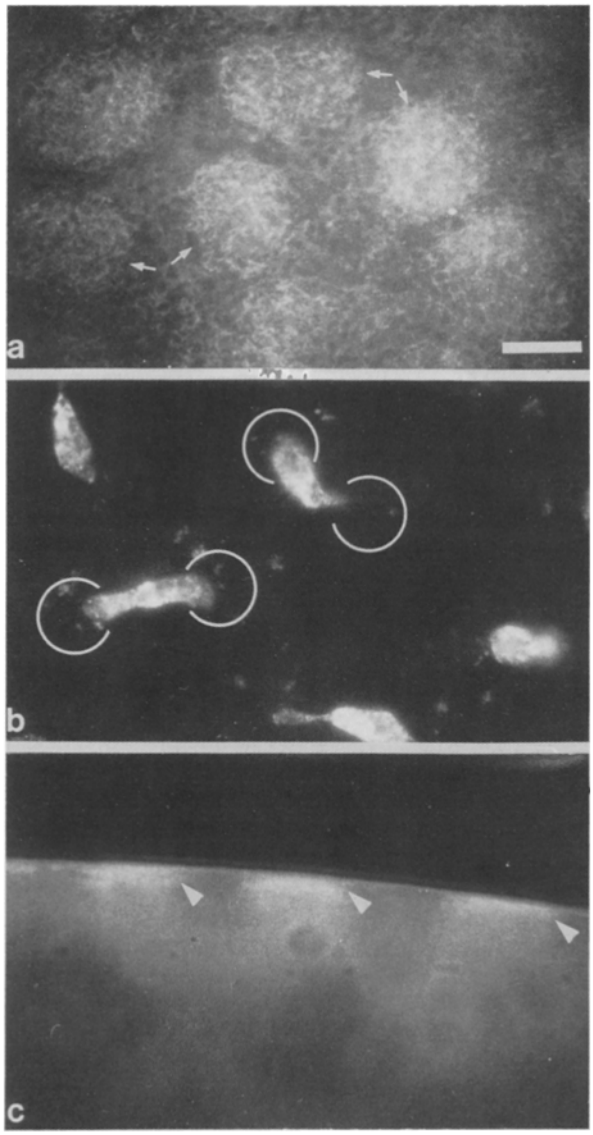

Figure 2. Spectrin cap formation. (*a*) Whole mount nuclear cycle 9 embryo, face view, showing several pairs of forming spectrin caps (*arrows*). (*b*) Same area as in *a*, but at a slightly lower plane of focus in the cytoplasm. Hoechst fluorescence to show the anaphase and telophase figures that underlie the pairs of caps in *a*. The white circles were drawn to be concentric with the overlying caps shown in *a*. The nuclei at left have nearly completed their movement to the embryo surface, whereas those at the upper right are still in the process of migrating to the surface. Thus, the poles of the mitotic figure in the lower left lie on a line that is parallel to the embryo surface; those at upper right lie on a line that is still at an angle to the embryo surface, as are several adjacent figures. (*c*) Parasagittal view of embryo in *a* to show spectrin caps (*arrowheads*) near the plasma membrane and the low levels of spectrin between caps. Spectrin is also concentrated in the cytoplasmic islands beneath each cap. Bar: (*a–c*) 10 μm.

(Karr and Alberts, 1986). A few embryos have spectrin caps at anaphase 9, others at telophase 9 (Fig. 2 *b*), and all do by the end of interphase 10. Many of the caps form as the nuclei are in the process of approaching the embryo surface (Fig. 2 *b*). Although the timing of cap formation varies from em-

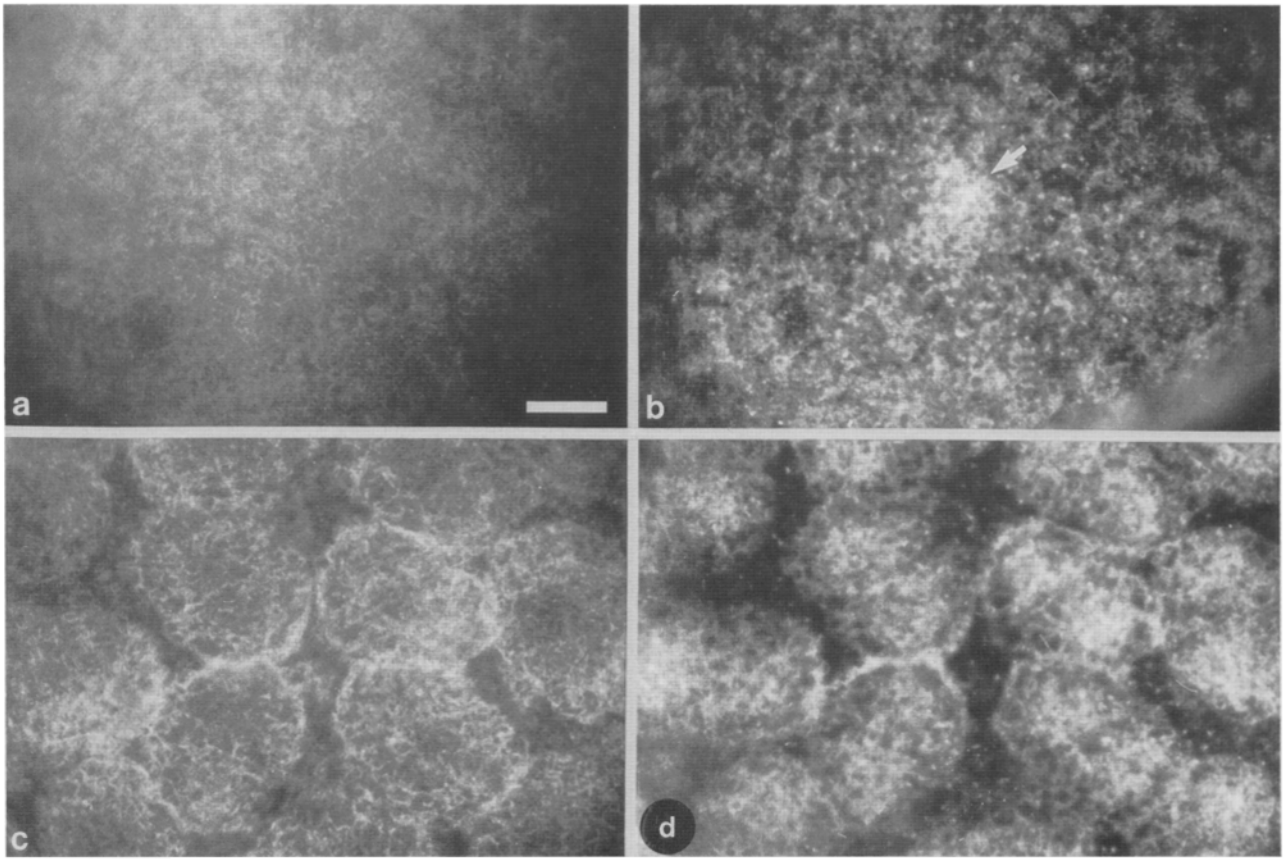

Figure 3. Spectrin and actin colocalization. Whole mount embryos double labeled for spectrin and actin. (*a*) Spectrin fluorescence at the surface of a nuclear cycle 9 embryo showing no spectrin caps. (*b*) Same area as in *a*, but actin fluorescence (anti-actin antibody). The actin caps (*arrow*) originate as small structures that do not all form simultaneously in each embryo. (*c*) Spectrin fluorescence at the surface of a syncytial blastoderm embryo during metaphase. (*d*) Same area as in *c*, but actin fluorescence. Bar: (*a–d*) 10 μm.

bryo to embryo, the movement of spectrin into caps must be abrupt: partially formed spectrin caps are rarely seen, and <15 min elapses between the beginning of anaphase 9 and the end of interphase 10 (Foe and Alberts, 1983). In face view, each cap is circular or sometimes slightly elliptical (Fig. 2 *a*), with an average diameter of 15 μm (n = 10; SD = 1.7 μm). A nucleus or mitotic figure is located in the cytoplasm below each cap (Fig. 2 *b*). In sagittal optical sections (Fig. 2 *c*), the amount of spectrin between the caps appears to be less than was present before cap formation, as though preexisting spectrin had relocated and concentrated to form the caps (compare Fig. 1 *e* with Fig. 2 *c*).

Antispectrin and antiactin antibodies were used in double-labeled embryos to evaluate the association of spectrin and actin. Before nuclear cycle 9, actin is present throughout the embryo at low levels and is concentrated uniformly near the plasma membrane, as previously described (Karr and Alberts, 1986; Warn and Magrath, 1983). Our results show that actin caps form before the time reported by Karr and Alberts (1986), appearing between anaphase 9 and early interphase 10. Although spectrin caps begin to form at this time, small actin caps are consistently present before spectrin cap formation (Fig. 3, *a* and *b*). Once formed, the two proteins codistribute within each cap (Fig. 3, *c* and *d*).

Nuclear Cycles 10–13 (from ~85 to 130 min): Spectrin Caps Elongate, Separate, and Collide with Other Caps

Although pseudo cleavage furrows form at each prometaphase during nuclear cycles 10–13, these furrows are transient and do not lead to cellularization (Stafstrom and Staehelin, 1984). During prophase 10, the centrosomes divide and move toward the eventual position of the spindle poles. Anticipating the division and directional movement of the chromosomes, the spectrin caps elongate during interphase and prophase, and the central portions of the elongated caps become narrowed (Fig. 4, *a* and *b*), presumably in the regions where daughter caps will separate from each other during the subsequent metaphase and anaphase (Fig. 4, *c* and *d*). Spectrin concentration in the region of incipient cleavage is no greater than in other regions of the cap. Thus, cap division does not appear to involve a constrictive or compressive mechanism, but rather an oppositely directed movement of daughter caps. During anaphase and telophase, the distance between daughter caps increases (Fig. 4 *e*) and their lineage becomes obscure. Inspection of the underlying Hoechst-stained telophase figures (Fig. 4 *f*) shows that in many cases the daughter caps collide with adjacent, nondaughter caps forming what appear to be slightly compressed areas of high spectrin concentration (Fig. 4 *e*). By interphase 11, the newly

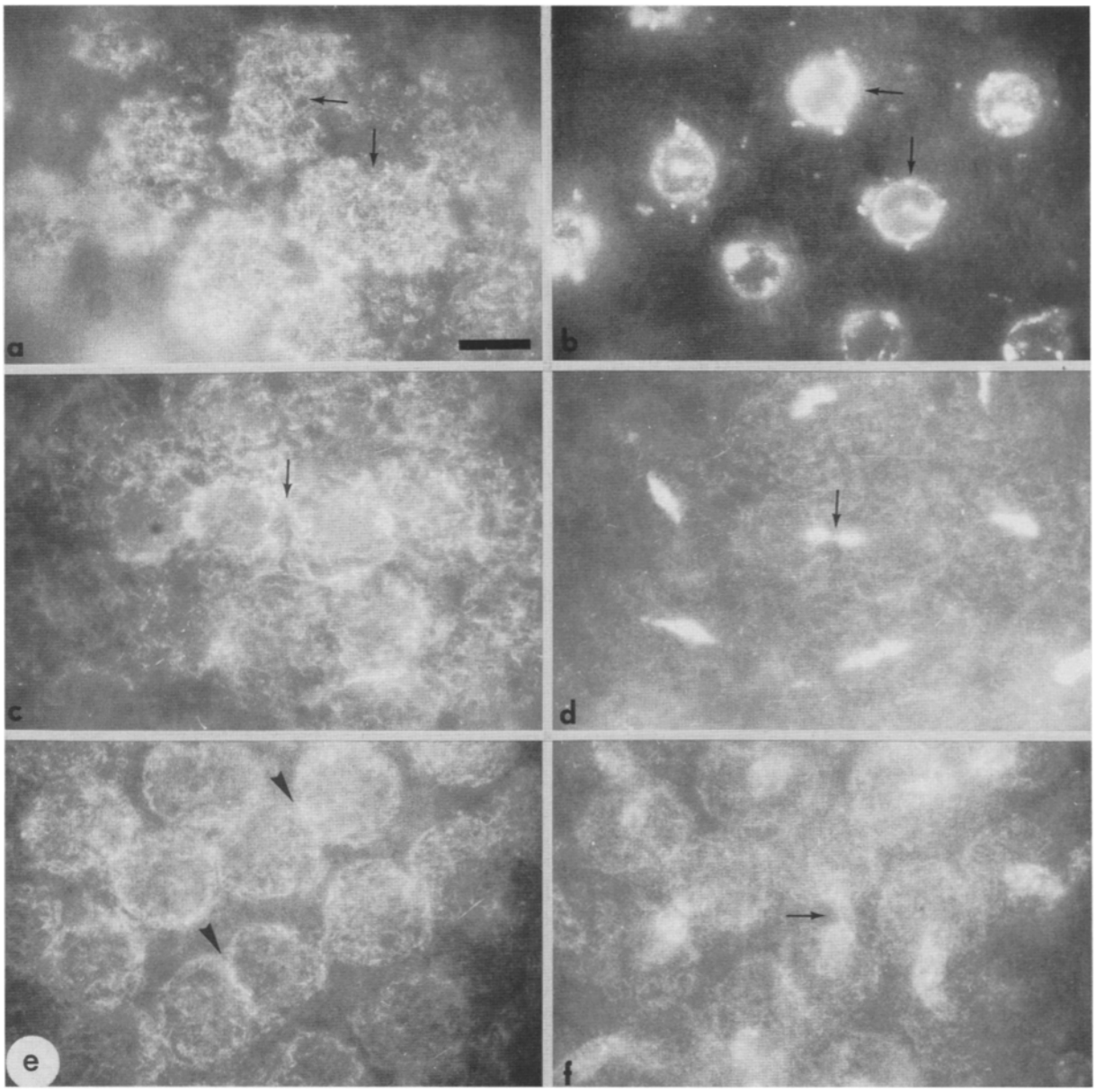

Figure 4. Spectrin caps during nuclear cycle 10 mitosis. Whole mount embryos double labeled with affinity-purified antispectrin antibody and Hoechst 33258. (*a*) Surface of embryo. The spectrin caps are elongated, with slight constrictions (*arrows*) visible between the forming daughter caps. (*b*) Same as in *a*, but illuminated to show Hoechst staining of late interphase nuclei (*arrows*) centered under the elongating spectrin caps in *a*. (*c*) Spectrin caps that are dividing (*arrow*). (*d*) Area in *c*, but double exposed to show Hoechst staining of anaphase figure (*arrow*) associated with the spectrin caps. (*e*) Spectrin caps colliding (*arrowheads*) after separation. (*f*) Double exposure of caps in *e* shows telophase figures (*arrow*) between daughter caps; and establishes the lineage relationship among caps. Bar: (*a–f*) 10 μm.

formed nuclei are generally centered under each cap. The apparent linkage between spectrin cap elongation, cap division, and karyokinesis is maintained during the next three rounds of mitosis, but becomes increasingly difficult to follow as the number of nuclei and caps increases and the distinction between cap and intercap regions is blurred. Although Warn et al. (1984) and Karr and Alberts (1986) report that the actin caps spread out and move into the pseudo furrows that form during the prophase–metaphase period of nuclear cycles 11–13, at no stage did we detect increased concentrations of spectrin near the pseudo cleavage furrows.

Interphase, Nuclear Cycles 11–13, and Pole Cell Development: Spectrin Is Concentrated in the Plasma Membrane and the Subjacent Cytoplasm

As the number of nuclei in a syncytial blastoderm stage embryo increases, nuclear size decreases (Zalokar and Erk, 1976). During interphase, the plasma membrane above each nucleus curves to produce an array of domes (Turner and Mahowald, 1976). Optical sections obtained with the scanning confocal microscope show that the distribution of spectrin follows the contour of the plasma membrane. Spectrin caps are no longer distinguishable, and spectrin fluorescence

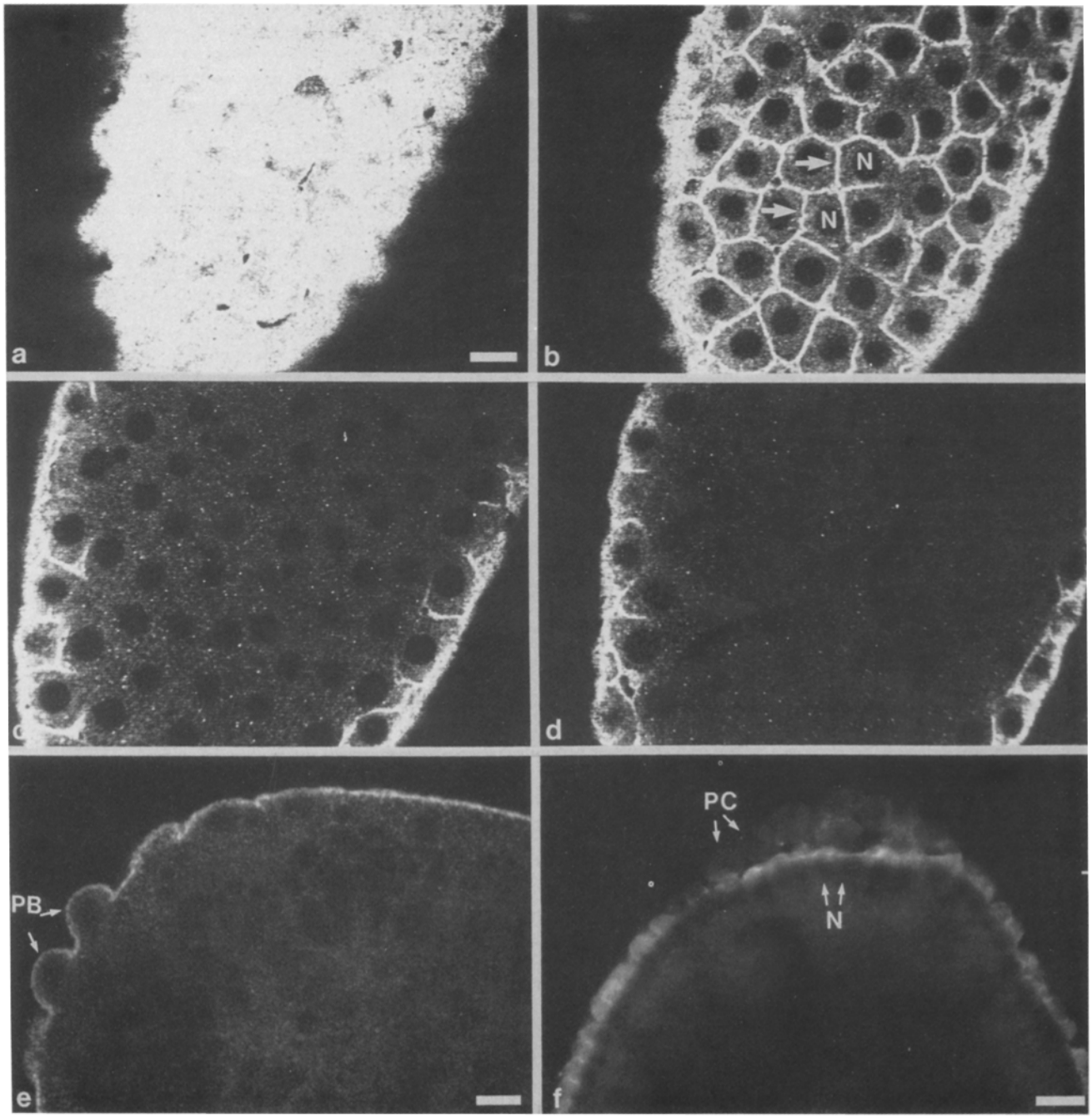

Figure 5. Syncytial blastoderm during interphase. (*a–d*) Successive scanning confocal microscope optical sections through part of a nuclear cycle 12 whole mount embryo. The optical sections are ~2 μm thick, and are taken at 4-μm increments, starting from the embryo surface in *a*. Arrows in *b* point to membrane-associated spectrin. Spectrin fluorescence is also clearly visible in the cytoplasm surrounding the nuclei (*N*). The concentration of spectrin in the cytoplasm diminished farther into the embryo (*c* and *d*) where the outlines of the nuclei and some yolk granules are difficult to detect. (*e*) Scanning confocal microscope optical section within a nuclear cycle 9 embryo whole mount. Spectrin is concentrated at the plasma membrane of pole buds (*PB*). (*f*) Cryosection of late syncytial blastoderm embryo. At this late syncytial stage, spectrin is present at the plasma membrane above the somatic nuclei (*N*), but is barely detectable at the plasma membrane of pole cells (*PC*). Bars: (*a–d*) 10 μm; (*e*) 7.5 μm; (*f*) 10 μm.

is uniform in *en face* optical sections of the surface of the embryo (Fig. 5 *a*). 4 μm farther into the same embryo, fluorescence encircles the nuclei of the syncytial blastoderm, but is greatest where the plasma membrane extends into the cytoplasm at the perimeter of each dome of plasma membrane (Fig. 5 *b*). Lesser concentrations of spectrin are evident in the cytoplasm between the unstained nuclei and the intensely stained plasma membrane (Fig. 5, *b* and *c*). At this stage of development, little or no spectrin is detectable near the yolk granules toward the center of the embryo (Fig. 5 *d*).

During nuclear cycle 9, spectrin distribution in the pole buds is similar to that found in the somatic regions (Fig. 5

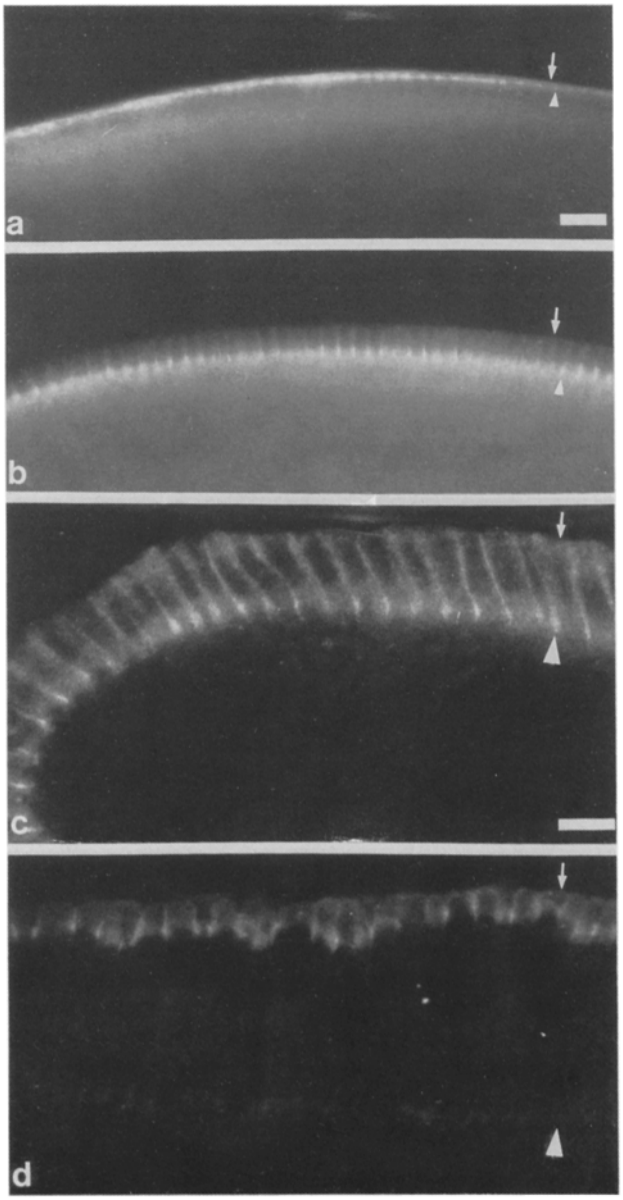

Figure 6. Cellularization. (*a*) Sagittal optical section through an embryo whole mount during the first (slow) stage of cellularization. Spectrin is concentrated near the furrow canals (*arrowhead*) which at this stage are close to the embryo surface (*arrow*). (*b*) Same as in *a*, but during the second (fast) stage of cellularization. The furrow canals have just passed the base of the elongated nuclei. The concentration of spectrin is highest just behind the advancing furrow canals (see Fig. 7, colocalization study with actin) with little spectrin at the embryo surface. (*c*) Cryosection of an embryo at a stage of cellularization similar to, or slightly later than, that in *b*. Spectrin is concentrated in the region near the furrow canals. (*d*) Cryosection of embryo in which cellularization is almost completed. The relative concentration of spectrin is now highest at the embryo surface, whereas spectrin near the furrow is almost undetectable. Bars: (*a* and *b*) 20 μm; (*c* and *d*) 10 μm.

e). Later, during the syncytial blastoderm stage, the amount of spectrin near the plasma membrane of pole cells begins to decrease (Fig. 5 *f*). Our observations of living embryos (Kiehart, D. P., P. E. Young, and S. Inoue, unpublished observations) indicate that the timing of this spectrin decrease varies somewhat from embryo to embryo, but, in general, coincides with a period of increased movement and microspike formation at the pole cell surfaces (not shown).

Cellularization (from ~130 to 170 min): Spectrin Shifts between the Furrow Canal and the Embryo Surface

After nuclear mitotic cycle 13, a distinctive period of cellularization occurs: each of the 5,000 or so cortical nuclei of the syncytial blastoderm, together with surrounding cytoplasm, is enclosed by plasma membrane to form the individual epithelial cells of the cellular blastoderm. This period is accompanied by striking changes in spectrin distribution. Immediately before cellularization, spectrin is uniformly concentrated near the plasma membrane. But during the first, slow phase of furrow growth (Fullilove and Jacobson, 1971), when many new microspikes appear at the embryo surface (Turner and Mahowald, 1976), the distribution of spectrin changes abruptly and becomes most concentrated near the furrow canal (Fig. 6 *a*). F-actin is also associated with the furrow canals, although a meshwork of actin filaments remains close to the cell apices (Warn and Magrath, 1983).

High concentrations of spectrin remain associated with the furrow until at least the beginning of the second phase of furrow growth, as the furrow proceeds deeper into the embryo and passes the elongated nuclei (Fig. 6, *b* and *c*). By this stage, there is less actin at the cell apices, and the F-actin associated with the developing lateral cell membranes is more densely packed (Warn and Magrath, 1983). Double-labeled preparations show that the region of highest actin concentration at the furrow canal is always slightly in advance of the most concentrated region of spectrin (Fig. 7, *a* and *b*). Late during this second phase of furrow growth, spectrin fluorescence almost disappears from the region near the furrow canal and becomes increasingly evident near the embryo surface (Fig. 6 *d*). Thus, within the 40-min period of cellularization, spectrin appears to cycle from the embryo surface, to the growing furrow, and then back again to the embryo surface. The return of spectrin to the embryo surface appears to coincide with the time during which the embryo surface becomes smooth (Turner and Mahowald, 1976) and the actin networks at the furrow tips become distinct, presumably contractile, rings (Warn and Magrath, 1983).

Gastrulation (from ~170 to 190 min): Spectrin Is Concentrated in the Apical Regions of the Epithelial Cells

Gastrulation is initiated during the terminal phase of cellularization. The relative concentration of spectrin near the embryo surface continues to increase during the early stage of gastrulation (Fig. 8 *a*), and immunofluorescence is brightest in distinct regions of the embryo, such as the developing amnioproctodeal invagination and the cephalic furrow (Fig. 8 *b*). To determine if these localized bright spots result from cell superposition, we immunostained 5-μm-thick cryosections of embryos that contained only a monolayer of cells. In these sections it is apparent that the cells of both the amnioproctodeal invagination and the cephalic furrow do indeed contain relatively high concentrations of spectrin in their apical regions (Fig. 8 *c*). In contrast, the pole cells showed lower levels of spectrin (Fig. 5 *f* and Fig. 9) where

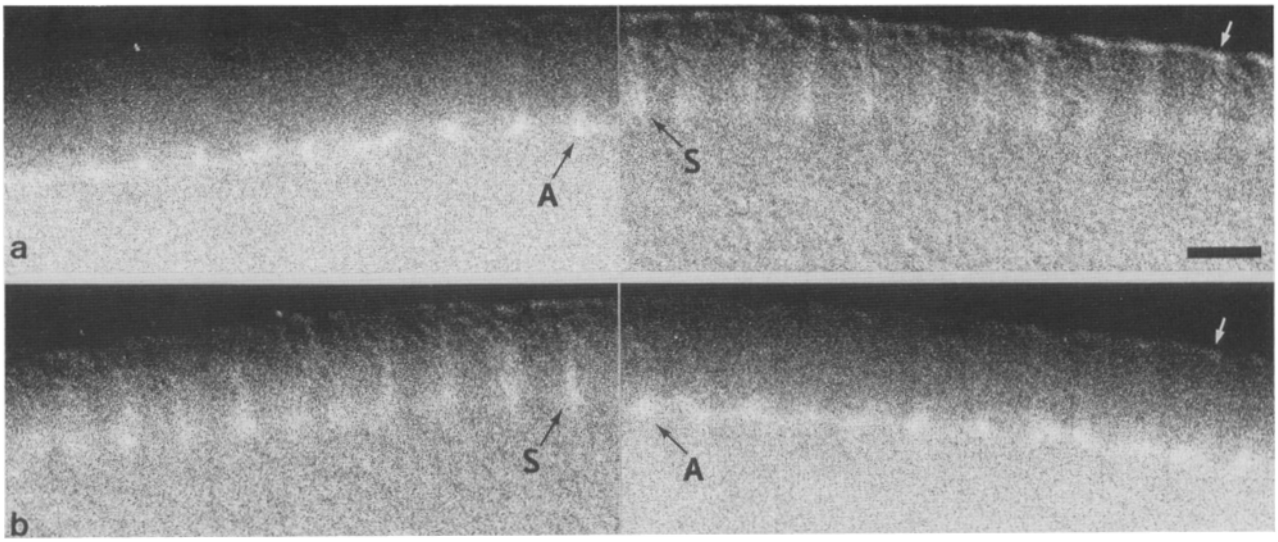

Figure 7. Double exposures (Nomarski/spectrin fluorescence or Nomarski/actin fluorescence) of cellularization. *a* and *b* are both montages produced from two prints taken at exactly the same focal plane in a whole mount embryo, one showing Nomarski/spectrin fluorescence, the other Nomarski/actin fluorescence. The Nomarski image, not fluorescence, illuminates the embryo surface (*white arrows*). Both prints were cut in two, on a vertical line through exactly the same place in the image. The right-hand side pieces were exchanged. *S*, spectrin; *a*, actin. It is clear that actin is located further from the embryo surface than spectrin. Bar, 5 μm.

double-label experiments (Fig. 9, *a* and *b*) clearly showed the presence of actin.

The localization of spectrin at the apical membranes of somatic cells during late cellularization and early gastrulation is in striking contrast to the more generalized distribution of spectrin around almost every cell in the embryo after just 1 h of further development (see below).

Postblastoderm Mitoses, Segmentation, and Later Development (from ~190 to 960 min): Spectrin Distribution Becomes Generalized

The end of gastrulation marks the beginning of the germband elongation stage. During the ensuing postblastoderm period of cell proliferation and tissue formation, spectrin becomes evenly distributed around the periphery of most cells (Fig. 10 *a*), but in amounts that vary from tissue to tissue. Thus, the spiracles and tracheal pits of the developing respiratory system contain high concentrations of spectrin (Fig. 10 *b*), whereas spectrin is difficult to detect in cells of the proventricular structure which joins the segments of the developing gut (Fig. 10 *a*). In addition to the peripherally localized spectrin, low concentrations of spectrin are diffusely distributed throughout the cytoplasm of both interphase and mitotic phase cells (Fig. 10, *c* and *d*). Although yolk granules are a major portion of the embryo, they never contain spectrin (Fig. 10 *a*).

Spectrin Accumulation during Embryogenesis

When immunostained embryos of different developmental stages are photographed together, it is evident that early embryos, including gastrulae, contain lower levels of spectrin immunofluorescence than do segmented embryos after germband shortening. Confocal optical sections through side-by-side embryos (Fig. 11 *a*) show that the greater fluorescence in the more mature embryos cannot be attributed simply to the superposition of cells. Rather, these optical sections suggest that the older embryos contain a greater amount of spectrin per unit surface area of plasma membrane than do the younger embryos.

Developmental immunoblots of whole embryo homogenates were used to quantify the changes in the level of spectrin during early embryogenesis. During the initial stages of development, up to and including gastrulation, the amount of spectrin per embryo remains approximately constant (Fig. 11 *b*). Immediately after gastrulation, as the cephalic furrow becomes the major visible morphological feature, the amount of spectrin begins to increase. The total amount of spectrin reaches a plateau as germband shortening occurs and segmentation becomes evident along the length of the embryo. This overall pattern of accumulation was duplicated in each of several experimental collections, but the proportional increase in spectrin varied between collections, with the amount of spectrin in late stage embryos being between 3.5- and 5.5-fold that found in the gastrula and pregastrula stages.

Using a known concentration of *Drosophila* alpha-spectrin as a standard, we calculate that late stage embryos contain on average 4.5 ng of alpha-spectrin per embryo. Assuming that such an embryo contains 40,000 cells and that the spectrin is equally distributed among them, each cell would contain $\sim 10^{-4}$ ng of alpha-spectrin. This represents $\sim 3 \times 10^5$ chains of alpha-spectrin/cell, a number remarkably close to the number of alpha chains in the 2.4×10^5 molecules of spectrin heterodimer in mature mammalian erythrocytes (Agre et al., 1985). A mammalian erythrocyte is comparable in size and surface area to a cell of the late stage *Drosophila* embryo.

Discussion

Our results show that during early *Drosophila* embryogenesis major events such as cellularization and gastrulation are

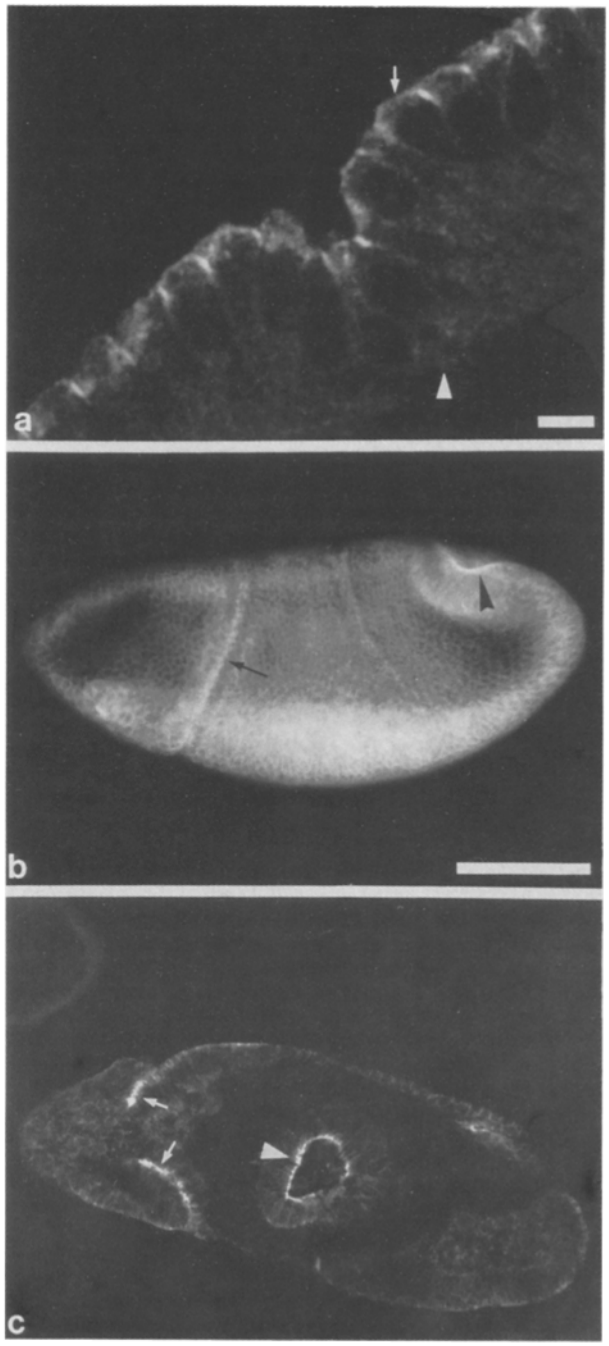

Figure 8. Gastrulation. (*a*) Whole mount showing an anterior transverse furrow and adjacent cells in a parasagittal optical section (scanning confocal microscopy). All of the cells show spectrin concentrated in the apical region (*arrow*); in contrast, basolateral membranes (*arrowhead*) contain no detectable spectrin. (*b*) Whole mount, sagittal optical section. Spectrin is concentrated at the surface of the forming amnioproctodeal invagination (*arrowhead*) and at the cephalic furrow (*arrow*). (*c*) Cryosection of an embryo in which germband elongation is at a later stage than in *b*, showing high concentrations of spectrin in the amnioproctodeal invagination (*arrowhead*) and the cephalic furrow (*arrows*). The pole cells enclosed by the amnioproctodeal invagination are difficult to detect because they contain very low levels of spectrin. Bars: (*a*) 10 μm; (*b* and *c*) 100 μm.

accompanied by striking, systematic changes in spectrin localization. Because the major formative events of early development occur during a period when the total amount of spectrin in an embryo does not increase, we infer that the accompanying localized changes in spectrin concentration in areas such as caps, furrow canals, or the apical regions of the gastrulating epithelial cells are probably the result of redistribution rather than de novo synthesis. This conclusion is consistent with the observation that the localized changes in spectrin concentration are rapid and that the accumulation of spectrin at one location often coincides with the diminution of spectrin at another. For example, the concentration of spectrin into caps coincides with a reduction of spectrin between the caps (compare Fig. 1 *e* with Fig. 2 *c*), and the deposition of spectrin near the apical surface of newly formed epithelial cells coincides with the diminution of spectrin at the basolateral regions of these cells (Fig. 6 *d*).

Observations of total spectrin during embryo development (Fig. 11) suggest that some of the developmental changes in spectrin localization involve the recruitment of unassembled maternal spectrin to the assembled state. Given the size of a *Drosophila* embryo and the average size of its cells, simple calculations show that the three rounds of postblastoderm mitoses that result in some 40,000 new cells must increase the total plasma membrane surface area at least 20-fold in comparison with the plasma membrane surface area in the syncytial embryo. Because the increase in membrane surface area substantially exceeds the 3.5–5.5-fold increment in total embryo spectrin (Fig. 11 *b*), the enhanced spectrin immunofluorescence at the plasma membrane of nearly all the cells produced by these postblastoderm mitoses (Fig. 11 *a*) cannot be accounted for exclusively by the increase in total spectrin. We therefore hypothesize that significant amounts of diffusely distributed, preexisting maternal cytoplasmic spectrin are recruited to the membrane during postblastoderm mitoses. If this hypothesis is correct, it implies that maternal spectrin can continue to play an important role in *Drosophila* development past the stages of embryogenesis examined here. We have begun to characterize several putative spectrin-deficient mutants. Their survival to the stage of third instar larvae is consistent with the sustained influence of maternal spectrin.

If diffusely distributed cytoplasmic maternal spectrin is recruited to cell surfaces and accounts for much of the fluorescence associated with the 20-fold increase of the plasma membrane surface area of postblastoderm embryonic cells, then cytoplasmic spectrin in the early syncytial stages (Figs. 1, 4, and 11) must represent a large fraction of embryonic spectrin. While spectrin is frequently defined as a plasma membrane–associated protein, our observations in *Drosophila*, as well as other observations in mammalian cells (Mangeat and Burridge, 1984; Nelson and Veshnock, 1987; Black et al., 1988), indicate that there can be important amounts of spectrin that are not associated with the cell surface. The diffuse appearance of this cytoplasmic immunofluorescence in comparison with the localized immunofluorescence at the embryo surface may easily lead to underestimates of the proportion of total spectrin in the cytoplasm.

Although spectrin caps appeared after actin cap formation, the spectrin caps always colocalized with the actin caps above the early syncytial-stage nuclei. Thus, spectrin was seen to concentrate in cytoplasmic domains that could be

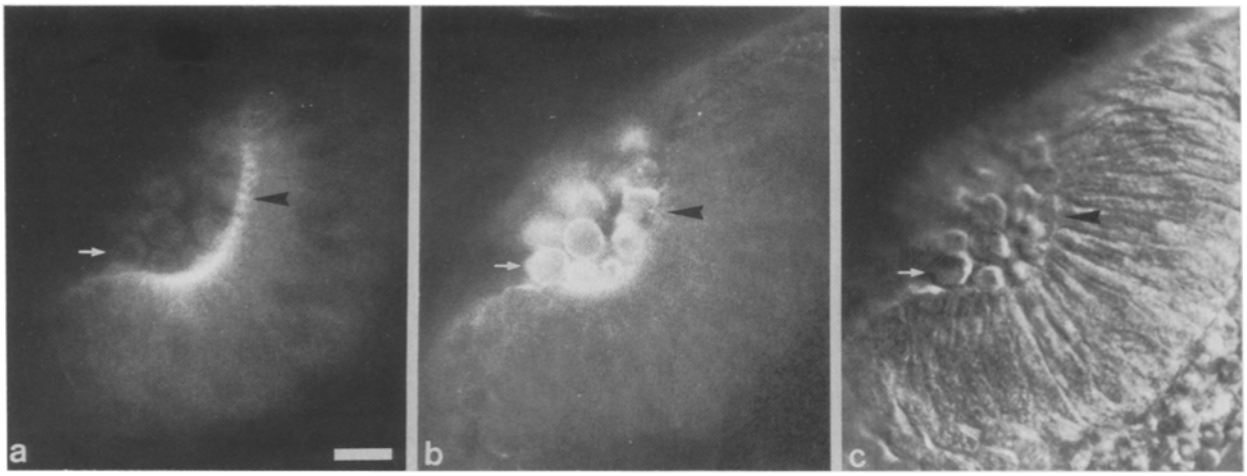

Figure 9. The forming amnioproctodeal invagination. Optical section in whole mount embryo double labeled for spectrin and actin. Pole cells (*arrows*) and the embryo surface (*arrowheads*). (*a*) Spectrin (antispectrin serum) is concentrated at the surface of the invagination and along very short portions of the lateral plasma membrane of each cell. Little spectrin is in the pole cells. (*b*) Actin (anti-actin antibody) is diffusely present near the surface of the embryo, including the amnioproctodeal invagination where spectrin is concentrated (see Fig. 8 *c*). Actin is more concentrated in the pole cells. (*c*) Nomarski micrograph of area in *a* and *b*. Bar, 10 μm.

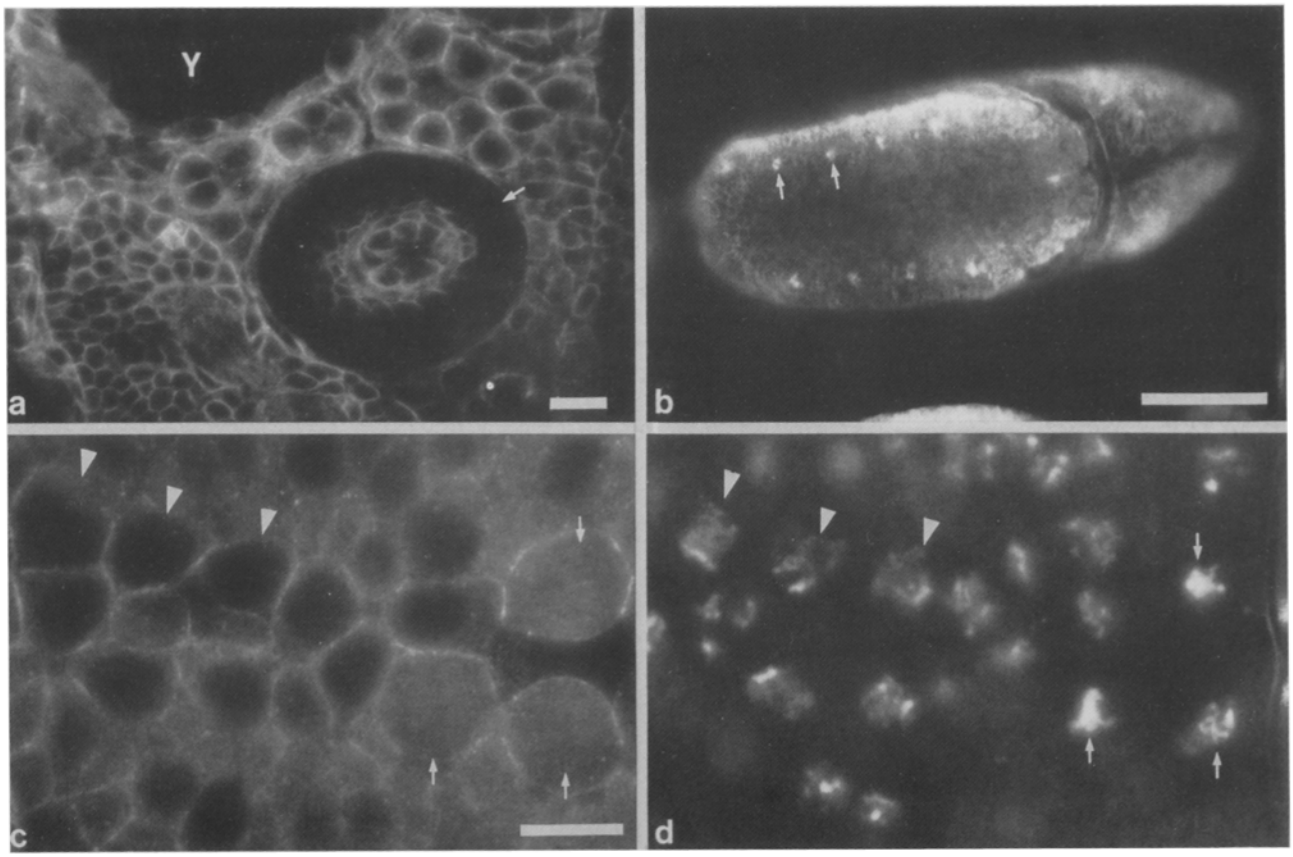

Figure 10. Late stages of development. (*a*) Cryosection of embryo interior showing spectrin (antispectrin serum) associated with many cell types except those of the proventriculus (*arrow*); control sections without antibody show that the area in the center of the proventriculus is autofluorescent (not shown). No spectrin is present in the yolk granules (*Y*). (*b*) Whole mount showing spectrin concentrated in the region of the trachae (*arrows*). (*c*) Whole mount, optical section near the embryo surface, showing prophase cells (*arrows*) in which spectrin is diffusely distributed throughout the cytoplasm; arrowheads indicate interphase cells in which spectrin is clearly absent from the nuclei. (*d*) Hoechst staining of embryo in *c* showing prophase figures (*arrows*) and interphase nuclei (*arrowheads*). Bars: (*a*) 10 μm; (*b*) 100 μm; (*c* and *d*) 10 μm.

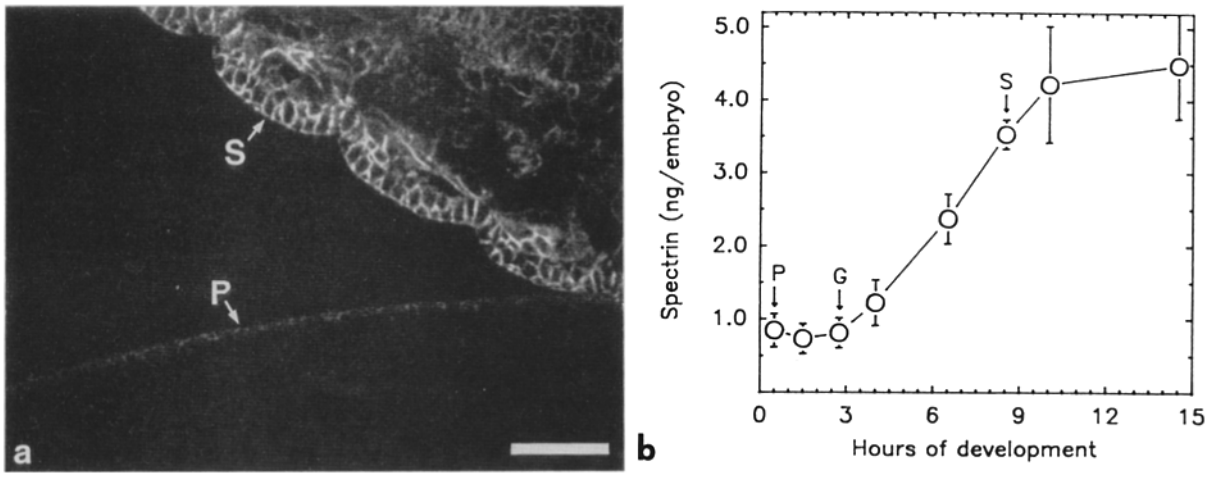

Figure 11. Spectrin content of embryos. (*a*) Scanning confocal microscope optical sections through a segmented, late stage embryo (*S*) and an adjacent preblastoderm embryo (*P*). Note the greater concentration of spectrin at the plasma membrane of the segmented embryo compared to that seen in the preblastoderm embryo. Bar, 30 μm. (*b*) Quantification of spectrin during development (see Materials and Methods). *P*, Preblastoderm embryo; *G*, gastrulating embryo; *S*, mid-point of segmentation and germband shortening. The great majority of postblastoderm mitoses occur between *G* and *S*. Error bars indicate ± 1 SD.

defined in terms of a temporally preexisting pattern of actin localization. Similarly, during cellularization, spectrin was localized behind the furrow canal, whereas actin (Warn et al., 1984; our observations) and myosin (Young, P. E., T. C. Pesacreta, and D. P. Kiehart, manuscript in preparation) colocalized in front of and around the advancing furrow canal. Here again, spectrin appeared to move into regions that could be defined by a previously existing pattern of high actin (and myosin) concentration. These and other examples showed that spectrin localization often succeeded rather than preceded other cytoskeletal changes during embryogenesis. We therefore reason that spectrin may frequently sustain or stabilize organization rather than initiate reorganization in *Drosophila* embryogenesis. We reason further that if the presence of spectrin stabilizes structure, its removal should facilitate structural change. Thus, the decrease of spectrin at the plasma membrane of pole cells during the syncytial blastoderm stage and the withdrawal of spectrin from the embryonic plasma membrane toward the lateral faces of the furrow canal during early cellularization may contribute to the simultaneous enhancement of membrane activity, such as microspike formation, that coincides with the diminution of spectrin at these membrane surfaces.

Despite spectrin's widespread occurrence and remarkably conserved structural features (Marchesi, 1985; Byers et al., 1987), its role in nonerythroid cells remains a puzzle. Although there is evidence that spectrin may maintain the physical state of the plasma membrane, modulate membrane lipid organization, stabilize membrane domain composition, or link cytoskeletal elements to the plasma membrane (Baines, 1984; Bourguignon et al., 1985; Harris et al., 1986; Nelson and Veshnock, 1986; Del Buono et al., 1988; Lee, J. K., J. D. Black, E. A. Repasky, R. T. Kubo, and R. B. Bankert, manuscript submitted for publication), one of the few experiments that attempted to directly assess spectrin's cellular function in nonerythroid cells did not produce data that supported an obvious role for this protein (Mangeat and Burridge, 1984). Our immunofluorescence studies in *Drosophila* extend knowledge of spectrin's localization to an invertebrate system in which a combination of genetic, molecular, and cell biological approaches should make it possible to clarify the precise functions of this protein.

The authors are grateful to Paul E. Young for his advice and generous help, to Drs. R. Daniel St. Johnston and Pedro Santamaria for their interpretations of morphology, and to Dr. Athar Husain-Chishti for his generous gift of erythrocyte spectrin.

This research was supported by National Institutes of Health grants GM 39686 to D. Branton and GM 33830 to D. P. Kiehart, and by a Postdoctoral Fellowship from the American Cancer Society to R. Dubreuil.

Received for publication 28 October 1988 and in revised form 22 December 1988.

References

Agre, P., J. F. Casella, W. H. Zinkham, C. McMillan, and V. Bennett. 1985. Partial deficiency of erythrocyte spectrin in hereditary spherocytosis. *Nature (Lond.).* 314:380–383.

Baines, A. J. 1984. A spectrum of spectrins. *Nature (Lond.).* 312:310–311.

Bennett, V. 1985. The membrane skeleton of human erythrocytes and its implications for more complex cells. *Annu. Rev. Biochem.* 54:273–304.

Black, J. D., S. T. Koury, R. B. Bankert, and E. A. Repasky. 1988. Heterogeneity in lymphocyte spectrin distribution: ultrastructural identification of a new spectrin-rich cytoplasmic structure. *J. Cell Biol.* 106:97–109.

Bourguignon, L. Y. W., S. J. Suchard, M. L. Nagpal, and J. R. Glenney, Jr. 1985. A T-lymphoma transmembrane glycoprotein (gp 180) is linked to the cytoskeletal protein fodrin. *J. Cell Biol.* 101:477–487.

Byers, T. J., R. Dubreuil, D. Branton, D. P. Kiehart, and L. S. B. Goldstein. 1987. *Drosophila* spectrin. II. Conserved features of the alpha-subunit are revealed by analysis of cDNA clones and fusion proteins. *J. Cell Biol.* 105:2103–2110.

Campos-Ortega, J. A., and V. Hartenstein. 1985. The Embryonic Development of *Drosophila melanogaster*. Springer-Verlag, Berlin. 1–227.

Del Buono, B. J., P. L. Williamson, and R. A. Schlegel. 1988. Relation between the organization of spectrin and of membrane lipids in lymphocytes. *J. Cell Biol.* 106:697–703.

Dubreuil, R., T. J. Byers, D. Branton, L. S. B. Goldstein, and D. P. Kiehart. 1987. *Drosophila* spectrin. I. Characterization of the purified protein. *J. Cell Biol.* 105:2095–2102.

Elgsaeter, A., B. T. Stokke, A. Mikkelsen, and D. Branton. 1986. The molecular basis of erythrocyte shape. *Science (Wash. DC).* 234:1217–1223.

Foe, V. E., and B. M. Alberts. 1983. Studies of nuclear and cytoplasmic behavior during the five mitotic cycles that precede gastrulation in *Drosophila* embryogenesis. *J. Cell Sci.* 61:31–70.

Fullilove, S. L., and A. G. Jacobson. 1971. Nuclear elongation and cytokinesis

in *Drosophila montana*. *Dev. Biol.* 26:560–577.
Glenney, J. R., Jr., P. Glenney, and K. Weber. 1982. F-actin-binding and cross-linking properties of porcine brain fodrin, a spectrin-related molecule. *J. Biol. Chem.* 257:9781–9787.
Harris, A. S., J. P. Anderson, P. D. Yurchenco, L. A. D. Green, K. J. Ainger, and J. S. Morrow. 1986. Mechanisms of cytoskeletal regulation: functional and antigenic diversity in human erythrocyte and brain beta spectrin. *J. Cell. Biochem.* 30:51–69.
Ishikawa, M., H. Murofushi, and H. Sakai. 1983. Bundling of microtubules *in vitro* by fodrin. *J. Biochem. (Tokyo).* 94:1209–1217.
Karr, T. L., and B. M. Alberts. 1986. Organization of the cytoskeleton in early *Drosophila* embryos. *J. Cell Biol.* 102:1494–1509.
Langley, R. C., Jr., and C. M. Cohen. 1986. Association of spectrin with desmin intermediate filaments. *J. Cell. Biochem.* 30:101–109.
Lazarides, E., W. J. Nelson, and T. Kasamatsu. 1984. Segregation of two spectrin forms in the chicken optic system: a mechanism for establishing restricted membrane-cytoskeletal domains in neurons. *Cell.* 36:269–278.
Lessard, J. L. 1988. Two monoclonal antibodies to actin: one generally reactive and one muscle-specific. *Cell Motility and the Cytoskeleton.* 10:349–362.
Mangeat, P. K., and K. Burridge. 1984. Immunoprecipitation of non-erythrocyte spectrin within live cells following microinjection of specific antibodies: relation to cytoskeletal structures. *J. Cell Biol.* 98:1363–1377.
Marchesi, V. T. 1985. Stabilizing infrastructures of membranes. *Annu. Rev. Cell Biol.* 1:531–561.
Nelson, W. J., and P. J. Veshnock. 1986. Dynamics of membrane-skeleton (fodrin) organization during development of polarity in Madin-Darby canine kidney epithelial cells. *J. Cell Biol.* 103:1751–1765.
Nelson, W. J., and P. J. Veshnock. 1987. Modulation of fodrin (membrane skeleton) stability by cell-cell contact in Madin-Darby canine kidney epithelial cells. *J. Cell Biol.* 104:1527–1537.
Olmstead, J. B. 1981. Affinity-purification of antibodies from diazotized paper blots of heterogeneous protein samples. *J. Biol. Chem.* 256:11955–11957.
Schatten, H., R. Cheney, R. Balczon, M. Willard, C. Cline, C. Simerly, and G. Schatten. 1986. Localization of fodrin during fertilization and early development of sea urchins and mice. *Dev. Biol.* 118:457–466.
Sobel, J. S., and M. A. Alliegro. 1985. Changes in the distribution of a spectrin-like protein during development of the preimplantation mouse embryo. *J. Cell Biol.* 100:333–336.
Sobue, K., T. Okabe, K. Kadowaki, K. Itoh, T. Tanaka, and Y. Fujio. 1987. Cytosynalin: an M_r 35,000 cytoskeleton-interacting and calmodulin-binding protein. *Proc. Natl. Acad. Sci. USA.* 84:1916–1920.
Stafstrom, J. P., and L. A. Staehelin. 1984. Dynamics of the nuclear envelope and of nuclear pore complexes during mitosis in the *Drosophila* embryo. *Eur. J. Cell Biol.* 34:179–189.
Tokuyasu, K. T., R. Schekman, and S. J. Singer. 1979. Domains of receptor mobility and endocytosis in the membranes of neonatal human erythrocytes and reticulocytes are deficient in spectrin. *J. Cell Biol.* 80:481–486.
Turner, F. R., and A. P. Mahowald. 1976. Scanning electron microscopy of *Drosophila* embryogenesis. *Dev. Biol.* 50:95–108.
Warn, R. M., and R. Magrath. 1983. F-actin distribution during the cellularization of the *Drosophila* embryo visualized with Fl-Phalloidin. *Exp. Cell Res.* 143:103–114.
Warn, R. M., R. Magrath, and S. Webb. 1984. Distribution of F-actin during cleavage of the *Drosophila* syncytial blastoderm. *J. Cell Biol.* 98:156–162.
Warn, R. M., L. Flegg, and A. Warn. 1987. An investigation of microtubule organization and functions in living *Drosophila* embryos by injection of a fluorescently labeled antibody against tyrosinated alpha-tubulin. *J. Cell Biol.* 105:1721–1730.
Zalokar, M., and I. Erk. 1976. Division and migration of nuclei during early embryogenesis of *Drosophila melanogaster*. *J. Micros. Biol. Cell.* 25:97–106.